

Discriminating Drug-Induced Ventricular Fibrillation via Wavelet Transforms and Deep Temporal Models

Dafne Lozano-Paredes¹, Luis Bote-Curiel¹, Juan José Sánchez-Muñoz²,
Francisco M Melgarejo-Meseguer¹, F Javier Gimeno-Blanes³, José Luis Rojo-Álvarez¹

¹ Department of Signal Theory and Communications. Universidad Rey Juan Carlos, Spain

² Arrhythmia and Electrophysiology Unit, Hospital Universitario Virgen de la Arrixaca, Spain

³ Department of Signal Theory and Communications. Universidad Miguel Hernández, Spain

Abstract

Ventricular fibrillation (VF) is a life-threatening arrhythmia whose electrophysiological characteristics vary under different pharmacological interventions. We propose a deep learning framework combining wavelet-based representations with time-aware modeling to classify VF episodes induced by amiodarone, diltiazem, flecainide, or no drug. Using electrocardiogram recordings from anesthetized dogs, we extract features via Continuous (CWT) and Scattering (SWT) wavelet transforms, and train Long Short-Term Memory networks to capture temporal dynamics. Classification performance is evaluated across VF segments, and latent representations are visualized. Results show improved separability over time, with SWT models outperforming CWT and achieving up to 68% macro F1-score on an independent test set. This score reflects physiological similarities between drug effects, particularly the consistent overlap between amiodarone and flecainide in classification and latent space. These findings highlight the value of interpretable, time-aware models for VF characterization analysis.

1. Introduction

Ventricular fibrillation (VF) is a life-threatening arrhythmia characterized by chaotic electrical activity and rapid, irregular contractions of the ventricles [1]. Its timely detection and classification are critical for clinical decision-making [2]. Antiarrhythmic drugs such as amiodarone, diltiazem, and flecainide exert different electrophysiological effects during VF, which can influence both the morphology and dominant frequency of the electrocardiogram (ECG) signal [3].

Previous studies have analyzed the frequency evolution of VF under drug intervention, highlighting time-dependent changes in dominant frequency [3]. While recent approaches have used more advanced signal analysis

[4], many still rely on manually extracted features and lack temporal modeling. Wavelet transforms offer a flexible way to capture non-stationary dynamics [5], and improve over fixed-window spectral methods. However, these representations are typically used within conventional processing frameworks that lack end-to-end temporal modeling.

In this work, we propose a deep learning-based framework for characterizing VF episodes induced by different pharmacological agents in a controlled experimental setting. We scrutinize both continuous and scattering wavelet transforms to extract time-frequency features, and train Long Short-Term Memory (LSTM) networks to learn temporal patterns directly from raw signals. By analyzing both classification performance and the structure of the learned latent space, we show that our model captures drug-specific characteristics that evolve throughout the VF episode, contributing to a better understanding of VF mechanisms.

2. Materials and Methods

2.1. Continuous Wavelet Transform

To extract time-frequency features, we applied the continuous wavelet transform (CWT) to each ECG signal \mathbf{x}_i , using a filter bank with frequency limits between 1 and 20 Hz. The CWT of a signal $x_i(t)$ is defined as:

$$W_x(a, b) = \frac{1}{\sqrt{|a|}} \int_{-\infty}^{\infty} x_i(t) \psi^* \left(\frac{t-b}{a} \right) dt, \quad (1)$$

where $\psi(t)$ is the Morlet wavelet, a the scale, and b the time shift.

The resulting CWT coefficients $W_x(a, b) \in \mathbb{C}$ form a complex-valued matrix $\mathbf{C}_i \in \mathbb{C}^{F \times T}$, where F is the number of frequency channels and T is the number of time steps. The magnitude $|\mathbf{C}_i| \in \mathbb{R}^{F \times T}$ was used as the input feature map for the deep learning models.

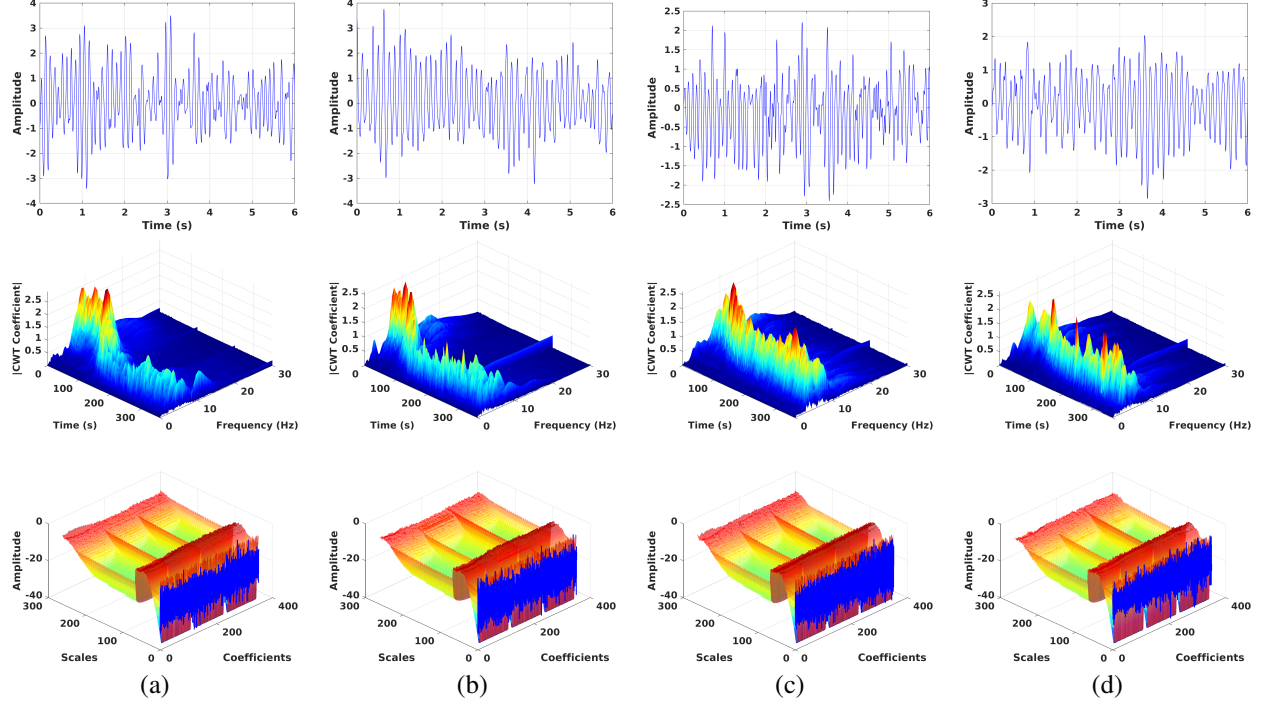


Figure 1. Top: 6-second ECG segments. Middle: CWT scalograms. Bottom: SWT coefficient surfaces. (a) Amiodarone, (b) Flecainide, (c) Diltiazem, (d) Control.

2.2. Scattering Wavelet Transform

The scattering transform produces stable, hierarchical features through cascaded wavelet modulus and low-pass filtering. For a signal $x_i(t)$, the first and second-order coefficients are:

$$S_1 x_i(t) = |x_i(t) * \psi_{\lambda_1}| * \phi(t), \quad (2)$$

$$S_2 x_i(t) = ||x_i(t) * \psi_{\lambda_1}| * \psi_{\lambda_2}| * \phi(t), \quad (3)$$

where ψ_{λ} are wavelets at scale λ , $\phi(t)$ is a low-pass filter, and $*$ denotes convolution.

The resulting scattering coefficients were averaged and stacked into a feature vector $s_i \in \mathbb{R}^D$, where D is the dimensionality of the scattering representation. These vectors were stacked into a matrix $\mathbf{S} \in \mathbb{R}^{N \times D}$, which served as input for the deep learning models.

2.3. LSTM-Based Classification

We trained LSTM neural networks to classify VF episodes based on wavelet-derived features. Two parallel models were implemented: CWT-LSTM and SWT-LSTM.

In the CWT-LSTM setup, each input $C_i \in \mathbb{R}^{F \times T}$, obtained from the continuous wavelet transform, was treated as a multivariate time sequence with F frequency bands and T time steps. In the SWT-LSTM configuration, fixed-length scattering vectors $s_i \in \mathbb{R}^D$ were first processed by

a fully connected layer and then passed through a shallow LSTM to capture internal structure among scattering paths.

Both models consisted of two or three stacked LSTM layers with a hidden state size h , followed by a dense ReLU layer and a softmax output layer. Training used the Adam optimizer with categorical cross-entropy loss. Classification performance was evaluated using accuracy, precision, recall, and F1-score across all classes.

2.4. Manifold Learning and Visualization

To visualize the internal representations learned by the LSTM models, we applied Uniform Manifold Approximation and Projection (UMAP) to the final hidden states. This nonlinear embedding method enabled qualitative assessment of class separability in the learned feature space.

2.5. Dataset

The dataset consists of $N = 23$ single-lead ECG recordings from anesthetized mongrel dogs with pharmacologically induced VF (amiodarone, diltiazem, flecainide, or control). VF was induced by right-ventricular catheter pacing with 2-s trains of 2-ms pulses (20–50 Hz) at five times the diastolic threshold [3]. Each recording lasts six minutes, sampled at $f_s = 1000$ Hz. Each signal was divided into three 2-minute segments: beginning, middle, and end. We denote the dataset as $\mathbf{X} \in \mathbb{R}^{N \times T}$, where each

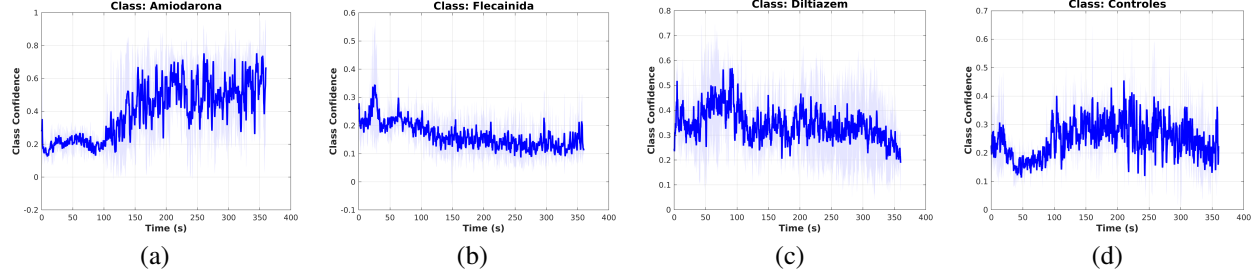


Figure 2. Class confidence trajectories across time with LSTM for each drug condition using CWT as input features.

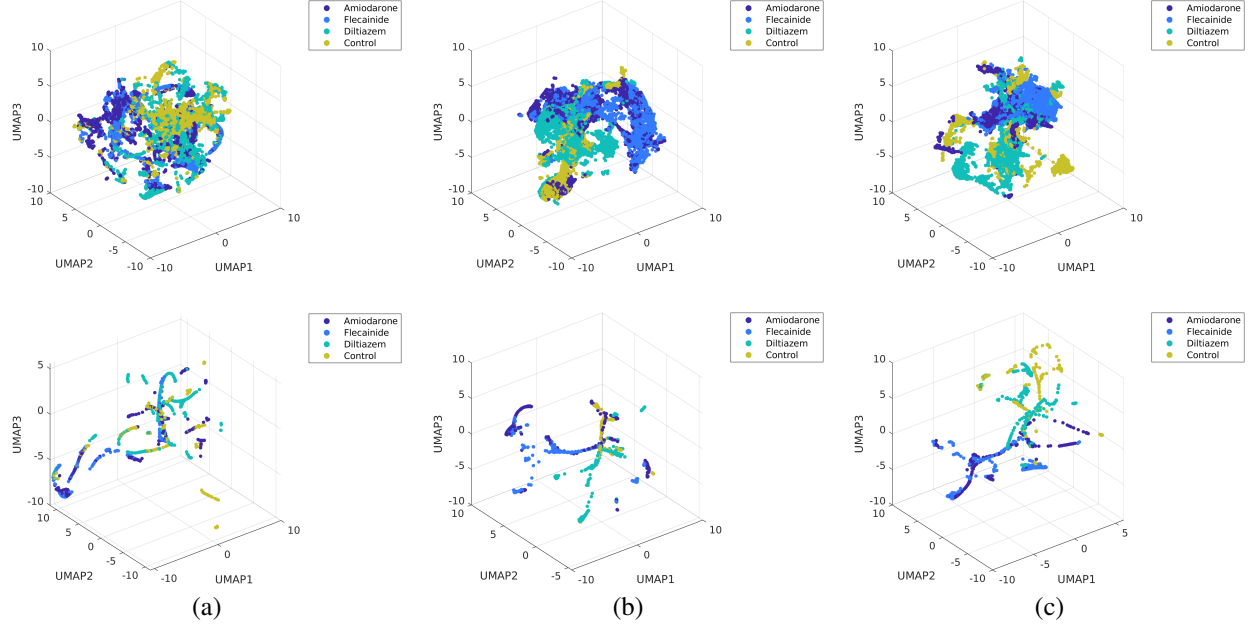


Figure 3. 3D UMAP projections of LSTM activations from CWT (top) and SWT (bottom). Columns: (a) Beginning, (b) Middle, (c) Ending. Colors indicate drug intervention class.

row $\mathbf{x}_i = x_i(t)$ is one individual ECG recording. No additional preprocessing was applied before wavelet-based feature extraction.

3. Experiments and Results

Figure 1 shows representative 6-second ECG segments from each drug condition, which serve as input to the wavelet-based feature extraction pipelines. CWT scalograms reveal evolving time-frequency patterns, while SWT surfaces capture hierarchical structures that reflect local and scale-dependent signal structures.

To assess temporal evolution, we tracked class probabilities over the 6-minute recordings as shown in Figure 2, in which the trained LSTM with CWT becomes more discriminative after the midpoint of the signal. To further explore this time-dependent behavior, we further divided each signal into three 2-minute segments and projected the LSTM activations using UMAP (Figure 3). Early seg-

ments showed high class overlap, whereas separation improved in later segments; amiodarone and flecainide consistently overlapped. Classification performance was evaluated on the coefficients of a test set from an 80/20 split of the 23 cases, which was not used for training or tuning. Table 1 summarizes the classification results across all three segments using CWT and SWT features. Accuracy and F1-score improve from early to late segments, with SWT models outperforming CWT, reaching a macro F1-score of 0.68. Finally, confusion matrices (Figure 4) summarize case-level predictions via majority vote across segments. Class overlap is most pronounced at the beginning of VF and between amiodarone (class 2) and flecainide (class 3), consistent with the latent space embeddings.

4. Discussion

Our findings align with previous studies showing time-evolving frequency dynamics in VF under different phar-

Table 1. Comparison of SWT and CWT Classification Metrics Across Signal Segments

Type	Metric/Class	S1 (SWT)	S1 (CWT)	S2 (SWT)	S2 (CWT)	S3 (SWT)	S3 (CWT)
Macro	Precision	0.395	0.370	0.456	0.640	0.692	0.660
	Recall	0.393	0.370	0.453	0.620	0.684	0.650
	F1-score	0.369	0.360	0.449	0.600	0.680	0.620
	Accuracy	0.403	0.390	0.451	0.610	0.683	0.630
Per-Class F1	Class 2	0.467	0.50	0.361	0.56	0.582	0.62
	Class 3	0.158	0.47	0.324	0.48	0.549	0.37
	Class 4	0.511	0.32	0.658	0.79	0.881	0.81
	Class 5	0.341	0.16	0.452	0.58	0.708	0.68

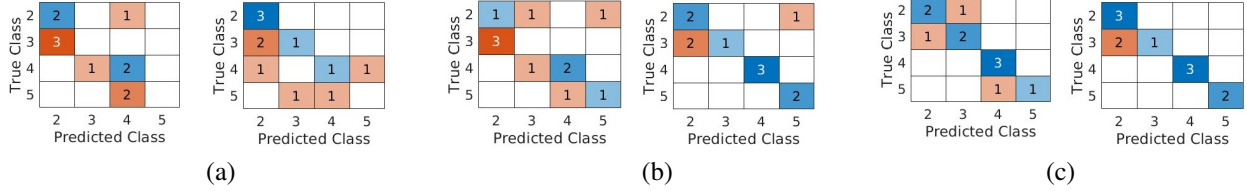


Figure 4. Confusion matrices by segment: (a) Beginning, (b) Middle, (c) End. Columns alternate CWT (left) and SWT (right). Class 2: Amiodarone, 3: Flecainide, 4: Diltiazem, 5: Control.

macological interventions. Diltiazem has been associated with increased dominant frequencies, while amiodarone and flecainide tend to slow arrhythmic activity [3]. These effects are reflected in our UMAP projections, where amiodarone and flecainide consistently overlap.

Unlike prior approaches based on predefined frequency markers, our method combines wavelet-based representations with LSTM networks to extract temporal and spectral features without manual segmentation or feature engineering. The improved classification performance in later VF segments suggests that drug-specific electrophysiological patterns become more distinct over time. By integrating deep learning with interpretable signal transformations, our study offers new insights into the evolving effects of antiarrhythmic drugs on VF morphology.

5. Conclusions

This study shows that time-aware deep learning models with wavelet-based features can effectively capture drug-specific patterns in VF. Temporal analysis improves classification, and latent space structure reveals different groups aligned with known electrophysiological effects. These findings support the use of interpretable, temporally structured models for VF characterization and drug response assessment.

Acknowledgements

This work was supported by Research Grants, LATENTIA, and PCardioTrials (PID2022-140786NB-C31, and PID2022-140553OA-C42) AEI/10.13039/501100011033

from the Spanish Ministry of Science and Innovation.

References

- [1] Gaztañaga L, Marchlinski FE, Betensky BP. Mechanisms of Cardiac Arrhythmias. *Revista Española de Cardiología English Edition* 2012;65(2):174–185.
- [2] Weiss JN, Garfinkel A, Karagueuzian HS, Nguyen TP, Olcese R, Chen PS, Qu Z. Perspective: A dynamics-based classification of ventricular arrhythmias. *Journal of Molecular and Cellular Cardiology* 2015;82:136–152. ISSN 0022-2828.
- [3] Chorro FJ, Sánchez-Muñoz JJ, Sanchis J, Cortina J, Bataller M, Guerrero J, Espí J, Ruipérez JA, López-Merino V. Modifications in the evolution of the dominant frequency in ventricular fibrillation induced by amiodarone, diltiazem, and flecainide: An experimental study. *Journal of Electrocardiology* 1996;29(4):319–326.
- [4] Bernal Oñate CP, Melgarejo Meseguer FM, Carrera EV, Sánchez Muñoz JJ, García Alberola A, Rojo Álvarez JL. Different ventricular fibrillation types in low-dimensional latent spaces. *Sensors* 2023;23(5).
- [5] Khadra L, Al-Fahoum AS, Al-Nashash H. Detection of life-threatening cardiac arrhythmias using the wavelet transformation. *Medical and Biological Engineering and Computing* Nov 1997;35(6):626–632.

Address for correspondence:

Dafne Lozano-Paredes. Dep. of Signal Theory and Communications. University Rey Juan Carlos, Madrid, Spain. Mail to: dafne.lozanop@urjc.es